



Insight into the effect of surfactant modification on the versatile adsorption of titanate-based materials for cationic and anionic contaminants

Wenlong Zhang^a, Xiaoyan Yang^a, Changzheng Lin^a, Jiangtao Feng^{a,*}, Hongjie Wang^b, Wei Yan^a

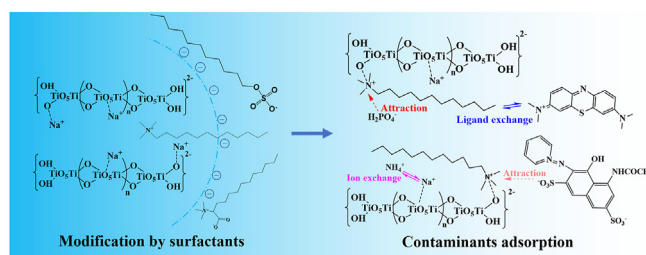
^a Department of Environmental Science and Engineering, State Key Laboratory of Multiphase Flow in Power Engineering, School of Energy and Power Engineering, Xi'an Jiaotong University, Xi'an, 710049, China

^b Xiong'an Institute of Eco-Environment, Institute of Life Science and Green Development, Hebei University, Baoding, 071002, China

HIGHLIGHTS

- Three types of surfactants were used to modify titanate-based materials.
- The versatile adsorption performance of modified materials was highly enhanced.
- Ion exchange is the main route for cationic contaminants removal.
- C–N⁺ from cationic surfactant is responsible for anionic contaminants adsorption.

GRAPHICAL ABSTRACT



ARTICLE INFO

Article history:

Received 9 October 2020

Received in revised form

13 December 2020

Accepted 17 December 2020

Available online 20 December 2020

Handling Editor: Junfeng Niu

Keywords:

Titanate
Surfactant modification
Versatile adsorption
Ammonia nitrogen
Phosphate
Organic dye

ABSTRACT

The new challenges to adsorption are imposed for the diversity of contaminants in wastewater in recent years. Herein, titanate-based materials (peroxide sodium titanate, PST) were modified by three different kinds of surface charged surfactant: dodecyl dimethyl betaine (BS-PST), sodium dodecyl sulphate (SDS-PST) and dodecyltrimethyl ammonium chloride (DTAC-PST) to enhance the versatile adsorption performance for four typical contaminants including ammonia nitrogen (NH₄⁺, inorganic and cationic), phosphate (H₂PO₄⁻, inorganic and anionic), methylene blue (MB, organic and cationic) and Acid Red G (ARG, organic and anionic). The batch adsorption experiments showed that the DTAC-PST exhibited better in the removal of MB, ARG and H₂PO₄⁻ than that of other adsorbents. The theoretical maximum adsorption capacity of DTAC-PST is 49.28 mg g⁻¹ for NH₄⁺, 34.74 mg g⁻¹ for TP, 81.87 mg g⁻¹ for MB and 545.81 mg g⁻¹ for ARG. The simultaneous adsorption results showed that the concentration (10 mg L⁻¹ of NH₄⁺, 3 mg L⁻¹ of TP, 50 mg L⁻¹ of MB and 50 mg L⁻¹ of ARG) of all the four chemicals in simulated wastewater could be controlled to be below the discharge levels in China (GB, 18918–2002) by DTAC-PST at the pH of 3.0. The FT-IR spectra demonstrated that ion exchange was the main way for NH₄⁺ removal, however, electrostatic attraction and ligand exchange were the reason for MB adsorption. In addition, C–N⁺ from DTAC modification made main contribution to the excellent adsorption performance for ARG and H₂PO₄⁻. The saturated DTAC-PST could be conveniently regenerated by 0.5 mol L⁻¹ NaOH solution and maintained about 80% of adsorption capacity after five cycles.

© 2020 Elsevier Ltd. All rights reserved.

* Corresponding author.

E-mail address: fjtes@xjtu.edu.cn (J. Feng).

1. Introduction

It is being witnessed that the human civilization in industrialization and urbanization progress greatly in the new century. The ever-increasing requirement for sustainable development has drawn intensive attention to the worldwide environmental issues like water pollution which can cause a direct risk to human health and ecological balance (Zhuang et al., 2019; Xu et al., 2020). Adsorption, one of the main physicochemical techniques for elimination of contaminants, has been frequently studied in research and used in engineering especially in advanced treatment of wastewater due to its high efficiency, cost effective and easy operation (Ye et al., 2019). However, the newly strict discharge levels and increasing complexity of effluent still call for the advance of existing adsorption technology (Schwarzenbach et al., 2010; Fu and Wang, 2011).

The various contaminants in industrial effluent contain organic and inorganic matters, the majority of which are cationic or anionic in nature (Wang and Peng, 2010). As a rule, the adsorption mechanism and performance of the same adsorbent for these contaminants is structure or surface chemistry dependent. Therefore, the increasing complicated components in wastewater undoubtedly affected the feasibility and efficiency of adsorption technique, which limited the future application of this method in water treatment (Crini et al., 2018). In order to strengthen the practicability of adsorption process, developing a versatile adsorbent for different kinds of contaminants in solution is one of the significant strategies. Nonetheless, the research about versatile adsorbent synthesis and evaluation is still short (Shen and Chen, 2015; Yu et al., 2017). For instance, Ammonia nitrogen (NH_4^+) and phosphate (H_2PO_4^- , one of the phosphorus forms in water) are typical inorganic matters in effluent with opposite surface ionization property, both of which make contribution to the eutrophication (Schindler et al., 2016; Wang et al., 2020). Methylene blue (MB) and Acid Red G (ARG), which are also inversely charged in solution, are typical organic compounds in industrial sewage (Shi et al., 2020). The adsorption of these four different kinds of typical contaminants (especially inorganic and organic together) onto one same adsorbent material was rarely focused on (Wang et al., 2016, 2020; Li et al., 2019; Xu et al., 2019).

It is necessary and significant to choose an optimal adsorbent material or modification method that can be applied in the simultaneously removal of cationic and anionic chemicals from water. There are few materials exhibiting well adsorption for more than two kinds of ammonia nitrogen, phosphate and dyes though several materials have excellent ability to adsorb single of above contaminants well, respectively (Wang et al., 2016; Wan et al., 2017b; Si et al., 2018). As a rule, the surface chemistry of adsorbent could play an important role in determining the adsorption interaction and adsorption capacity (Hokkanen et al., 2016). The negatively charged surface will tend to adsorb cationic matter in solution instead of the anionic one, and vice versa. Therefore, several modification methods have been used for adsorbent material to enhance the adsorption performance for some kind of contaminants (Wang et al., 2018b). Titanate-based material has been proved to be effective in the removal of most cationic chemicals (such as NH_4^+ and heavy metals) in aqueous phase due to its excellent ion exchange ability (Zhang et al., 2019; Zhao et al., 2019). In addition, the modification on titanate can be suitable and eco-friendly according to its facile preparation process and inorganic nature (Tan et al., 2018). The ion exchange property of titanate gives it potential in versatile adsorption because most modification methods have little effect on the ion exchange process (He et al., 2016; Wan et al., 2017a). Therefore, titanate was chosen as the primary material and served as adsorbent for different kinds of

contaminants after the modification.

Among the many modification methods for improvement of adsorption capacity, such as acid/base treatment, grafting of amine groups and impregnation of metals, the surfactant modification has gradually attracted considerable attention because of its facile operation and diversification (Rajapaksha et al., 2016; Li et al., 2018b; El Hanache et al., 2019). All the surfactants can be divided into non-ionic surfactant and ionic surfactant, and the latter one (cationic, anionic or ampholytic form) is more appropriate for the modification according to their ionization state in solution. Lots of ionic surfactants have been used for modification and proved effective in adsorption for various contaminants (Li et al., 2018a). The enhanced adsorption capacity was observed in adsorption of Cd^{2+} on amphoteric surfactant activated montmorillonite, the adsorption of methylene blue on anionic surfactant modified ZnFe_2O_4 , the adsorption of congo red on cationic surfactant modified pumice and so on (Liu et al., 2016; Shayesteh et al., 2016; Zhang et al., 2017). However, the effect of surfactant kind on the modification and versatile adsorption performance for different contaminant was rarely focused on. Therefore, three different kinds of typical surfactants were chosen as the modification reagent to improve the versatile adsorption capacity of titanate materials: ampholytic surfactant dodecyl dimethyl betaine (BS), anionic surfactant sodium dodecyl sulphate (SDS) and cationic surfactant dodecyltrimethyl ammonium chloride (DTAC). The pathway of how the adsorbent material is modified by surfactant and the relationship between the surfactant species and the adsorption capacity were focused on. The similar dodecyl structure and different ionic form of these surfactants can be conducive to study the modification and adsorption mechanism.

Based on the above discussions, the major purpose of this work is to: 1) facilitate synthesize the modified titanate materials with the three different kinds of surfactants and reveal the modification mechanism, respectively; 2) investigate their adsorption performance for individual chemical (NH_4^+ , H_2PO_4^- , ARG and MB) and evaluate the versatile adsorption ability for mixed contaminants through simultaneous adsorption experiments; 3) figure out the possible adsorption mechanism to understand the relationship between the surfactants property and adsorption performance.

2. Experimental

2.1. Chemicals

The titanium isopropoxide (TIPT, $\text{Ti}(\text{OC}_3\text{H}_7)_4$), hydrogen peroxide (H_2O_2 , 30 wt%), sodium hydroxide (NaOH), hydrochloric acid (HCl), dodecyl dimethyl betaine (BS), sodium dodecyl sulphate (SDS), dodecyltrimethyl ammonium chloride (DTAC) and isopropanol were of analytical grade. The simulated wastewater used in this study were obtained by dissolving ammonium chloride (NH_4Cl , GR), sodium dihydrogen phosphate ($\text{NaH}_2\text{PO}_4 \cdot 2\text{H}_2\text{O}$, AR), methylene blue (MB, AR) and acid red G (ARG, AR) into distilled water, respectively. All the chemicals and reagents were purchased from Sinopharm Chemical Reagent Co. Ltd, China and used as received. The deionized water used for all the experiments was prepared by an EPED-40TF Super pure Water System, China. The chemical structure of SDS, DTAC and BS are shown in Fig. S1 and chemical structure of MB and ARG are shown in Fig. S2.

2.2. Preparation of materials

Preparation of titanate-based materials. The titanate-based materials was synthesized according to the previous study (Zhang et al., 2019), and the typical way is as follows: a mixture of TIPT (10 mL) and isopropanol with the volume ratio of 5:2 was dropped

into 200 mL NaOH solution (0.1 mol L⁻¹) with magnetic stirring at 60 °C for 30 min. Subsequently, 10 mL of H₂O₂ (30 wt%) was added into the white suspension dropwise in 60 min. The solution gradually became yellow and then the suspension was stirred for another 30 min at 25 °C. After that, the resulting mixture was filtrated with the rinsing of deionized water until the pH value of the washing liquid reached about 7.0 and then dried in an oven at 60 °C for 12 h. The final obtained powder product was named as PST (peroxo sodium titanate) and used in the subsequent modification procedure.

Preparation of surfactant modified PSTs. The modification of PST was conducted in a 500 mL beaker: three surfactant solution with different concentration (1, 5 and 10 g L⁻¹) was prepared by dissolving one of the three surfactants into deionized water, respectively. A certain amount of PST powder was impregnated into the above nine as-prepared solution with magnetic stirring for 24 h, respectively. Afterward, the products were obtained through filtration and the rinse process was conducted with deionized water and alcohol sequentially. All the samples were then dried at 60 °C for 12 h and donated as BS-PST-1, BS-PST-5, BS-PST-10, SDS-PST-1, SDS-PST-5, SDS-PST-10, DTAC-PST-1, DTAC-PST-5 and DTAC-PST-10, respectively.

2.3. Characterizations

The morphology of the as-prepared samples was investigated by a scanning electron microscopy (SEM, MAIA3 LMH, USA) with the ancillary energy dispersive spectrometry (EDS). The element distribution and state of the materials were determined by X-ray photoelectron spectroscopy (XPS, Thermo Fisher ESCALAB Xi⁺, USA). The surface functional groups of the samples were identified by a fourier transform infrared spectrometer (FT-IR, Bruker, Germany). The zeta potential of the samples was measured with Brookhaven 90plus Zeta, samples of which (1.0 mg) were added into 10 mL NaCl solution (10⁻³ mol L⁻¹) at different pH values (adjusted by 0.5 M HCl or NaOH solution). Thermogravimetric analysis (TGA) was conducted at a heating rate of 10 °C·min⁻¹ to quantify the amount of surfactant loading on materials surface. The samples were heated from room temperature to 600 °C under nitrogen atmosphere and carried out on the SHIMADZU TA-60WS Thermal Analyzer.

The total NH₄⁺ concentration in the aqueous solution was determined by the conventional salicylate spectrophotometric method; the phosphate concentration was showed through the value of total phosphorus (TP) and measured by molybdenum antimony anti-colorimetric method; the concentration of MB and ARG in the solution was tested through the ultraviolet–visible spectrophotometry (UV2600, Shimadzu) directly.

2.4. Adsorption experiments

Unless otherwise stated, adsorption experiments were performed at 25 °C in a temperature-controlled shaker with a 200 rpm rate. The mixture after adsorption were separated by filtration through 0.45 µm filters.

The effect of surfactant dosage used in synthesis on the adsorption performance was investigated as follows: 0.04 g of surfactant modified sample (BS-PST-1, BS-PST-5, BS-PST-10, SDS-PST-1, SDS-PST-5, SDS-PST-10, DTAC-PST-1, DTAC-PST-5, DTAC-PST-10) and 20 mL of the simulant contaminant solution with pH of 7 was mixed in a 50 mL tube and shaken for 12 h, respectively. The adsorption experiment of PST was also conducted for comparison.

In order to know the effect of solution pH on the adsorption performance of the samples and find the influence of surfactant

modification, the initial pH value of the simulant contaminant solution was adjusted to the range of 2–10 by 0.5 mol L⁻¹ HCl or NaOH solution. The initial concentration of solution is 300 mg L⁻¹ for MB, 200 mg L⁻¹ for ARG, 40 mg NH₄⁺·L⁻¹ for NH₄⁺-N and 20 mg TP·L⁻¹ for phosphate. Only the samples modified by 5 g L⁻¹ surfactant (BS-PST-5, SDS-PST-5, DTAC-PST-5) were used in the batch experiments according to their comprehensive adsorption performance. The choice of optimal samples also alleviated the workload in adsorption experiment and kept the conditions constant. In addition, the adsorption performance of PST was also evaluated at the same condition for comparison.

Experiments to determine kinetics were carried out in a conical flask by adding 0.2 g of sample into 100 mL solution containing one of the contaminants with optimal solution pH according to the result of pH experiment. The initial concentration of solution is 300 mg L⁻¹ for MB, 200 mg L⁻¹ for ARG, 40 mg NH₄⁺·L⁻¹ for NH₄⁺-N and 20 mg TP·L⁻¹ for phosphate. About 1.5 mL mixed solution was collected at certain time intervals and filtered for the determination of the residual contaminant.

The isotherm adsorption experiments were conducted as follows: 0.04 g of adsorbent sample was added into a 50 mL centrifuge tube containing 20 mL individual adsorbate solution. The initial concentration for each contaminant was set as 10–120 mg L⁻¹ for NH₄⁺, 3–50 mg L⁻¹ for total phosphorus, 50–400 mg L⁻¹ for MB and 50–400 mg L⁻¹ for ARG, respectively. The mixture was shaken for 120 min in a temperature controlled shaker.

Simultaneous adsorption experiment was conducted to evaluate the adsorption performance of adsorbent for complex wastewater. The optimal samples were chosen as adsorbents according to batch adsorption experiment. The adsorption process was finished in mixed solution with different initial pH from 2.0 to 10.0. The initial concentration of contaminants was set as NH₄⁺ of 10 mg L⁻¹, TP of 3 mg L⁻¹, MB of 50 mg L⁻¹ and ARG of 50 mg L⁻¹ according to the actual condition before advanced treatment in wastewater treatment plant.

The stability or long-term performance of optimal adsorbent was determined by TGA after washing with deionized water or ionic solution (0.15 mol L⁻¹ NaCl solution) for 72 h. Desorption and regeneration of adsorbent was conducted by 0.5 mol L⁻¹ NaOH solution. The adsorption reusability experiment was carried out with the mixed solution containing 10 mg L⁻¹ NH₄⁺, 3 mg L⁻¹ TP, 50 mg L⁻¹ MB and 50 mg L⁻¹ ARG for five cycles.

There are some parameters and models used to evaluate and reveal the adsorption performance in this study. The adsorption efficiency η (%), the amount of matter adsorbed on the as-prepared adsorbents (adsorption capacity) at certain time Q_t (mg·g⁻¹) and at equilibrium Q_e (mg·g⁻¹) were calculated by Eqs. (1)–(3), respectively. Where C_0 (mg·L⁻¹), C_t (mg·L⁻¹) and C_e (mg·L⁻¹) are the initial concentration, residual concentration at time t (min) and residual concentration at equilibrium in the solution; m (g) is the adsorbent mass and V (L) is the solution volume. As shown in Eqs. (S1)–(S5), three kinetic models (pseudo-first order, pseudo-second order and elovich models) and two isotherm models (Langmuir model and Freundlich model) were used to analyze the adsorption data and reveal the adsorption process.

$$\eta = \frac{C_0 - C_t}{C_0} \times 100 \quad (1)$$

$$Q_t = \frac{C_0 - C_t}{m} \times V \quad (2)$$

$$Q_e = \frac{C_0 - C_e}{m} \times V \quad (3)$$

3. Results and discussion

3.1. Characterization

The facilely synthesized samples were observed under a scanning electron microscope. The SEM images (Fig. S3) illustrate that morphology of all the samples are particle-dominated and the diameter vary with experimental conditions. It is indicated that the particles of PST are in large scale with a smooth surface (Fig. S3a). The surfactant modification makes some of these particles fracture (Fig. S3b-j). The dispersed granules in modified samples could endow more active sites for adsorption than PST. The particles diameter of all the as-prepared samples are in the order of DTAC-PSTs < SDS-PSTs < BS-PSTs < PST. The change of morphology demonstrates that surfactant modification could affect the structure directing process of materials. Furthermore, the change degree of morphology varied with surfactant species and concentration also indicate the different combination form between PST substrate and the different surfactants.

The EDS and XPS results (Fig. S4-5) show that Ti, O and Na elements maintained in all the modified samples and indicate the stable structure. The content of C in DTAC-PST increases dramatically accompanies with the reduction of Na compares with the bare PST. The content of Na in BS-PSTs decreases lightly and the amount of Ti, O, Na in SDS-PSTs keep constant. In addition, the high resolution XPS results (Fig. S4c-d) show that there is S in SDS-PST-5 and N in BS-PST-5, respectively. The above results demonstrate that surfactant modification is successfully conducted. It is also found that DTAC surfactant impacts element content of PST more significantly than that of SDS and BS. Furthermore, the reduction of Na⁺ also indicates that the modification process might be associated with the existence or movement of Na⁺. The XPS high resolution of C1s and O1s for PST and the modified samples (Fig. S6) show that element valence state keep constant during the modification procedure. However, some shifts in C1s and O1s high resolution spectra of modified samples mean the change of surface charge in C and O and indicate that the electrostatic interaction probably occurs between PST and the surfactants.

Zeta potential of PST and the modified samples were tested to find the surface charge distribution and the results are shown in Fig. S7. It is observable that the surface of PST could be negatively charged at a wide pH range (pH > 1.52) and the isoelectric point (pH_{iep}) of PST slightly increases after modification. During the modification process, cationic groups would be attracted to the surface of PST more easily than anionic groups due to the electrostatic interaction. The relative cationic side of surfactant could move closer or attach to the PST particles. Therefore, it is more difficult for SDS and BS to attach on the surface of PST during modification than cationic DTAC.

The functional groups of PST and modified samples were investigated by FTIR, the spectra are showed in Fig. S8 and the attribution of peaks are listed in Table S1-S5. It is obvious that the modification by cationic DATC is more effective than that by BS or SDS. The peaks at 900 cm⁻¹ and 1340 cm⁻¹ representing Ti–O stretching mode appeared in all samples and demonstrate that the main structure of PST remained (Kiatkittipong et al., 2010; Turki et al., 2013). For SDS modified samples, the modification only had slight effect on PST according to the result that the spectra of SDS-PST-1, SDS-PST-5 and SDS-PST-10 are nearly consistent with that of

PST (Fig. S8b). The electrostatic repulsion between negatively charged PST and anionic SDS might cause the weak modification. The peaks in BS-PST samples are also similar with PST except that the peak attributed to C–O stretching vibration appeared at 1150 cm⁻¹ (Fig. S8a) (Wang et al., 2018c). The C–O bond is originated from the COO⁻ group in BS and its intensity increases with the amount of BS. However, the relative weak intensity of this peak also indicates that the modification by BS is limited. In the spectra of DTAC-PST samples (Fig. S8c), the peaks at 2930 cm⁻¹ (antisymmetric stretching vibration of CH₂), 2850 cm⁻¹ (symmetric stretching vibration of CH₂), 1470 cm⁻¹ (–C–H vibration of quaternary ammonium moiety), 720 cm⁻¹ (deformation vibration of CH₂ in long-chain alkanes (–(CH₂)_n–, n ≥ 4)) and 970 cm⁻¹ (stretching mode of C–N⁺) illustrate that DTAC has been successfully loaded into PST (Tang et al., 2016; Wang and Cao, 2018; Wang et al., 2018a). It is also observable that relative peak intensity at about 1340 cm⁻¹ corresponding to Ti–O bond decreases gradually along with the increase of DTAC amount. The Ti–O bond is demonstrated to interact with Na⁺ (Zhang et al., 2019). Therefore, the load of DTAC in PST would break this relationship and reduce the amount of Na⁺ as shown in EDS results (please see Fig. S4 and Fig. S5). In a word, DTAC probably moves close to PST through the electrostatic attraction and attaches in PST through occupying the sites of Na⁺.

3.2. Effect of surfactant dosage

The adsorption of four typical contaminants on PST and all the modified samples were conducted to find the effect of surfactants dosage on the adsorption performance, respectively. It is illustrated from Fig. 1 that the adsorption efficiency of these materials is generally in the order of DTAC-PSTs > BS-PSTs ≈ SDS-PSTs ≈ PST. The surfactant type and dosage could both make impacts on the adsorption performance of these contaminants. For inorganic NH₄⁺, the adsorption capacity of modified samples is nearly consistent with the bare PST at solution pH = 7. Among all the adsorbents, the BS-PSTs performed slightly better than that of others for the removal of NH₄⁺. The adsorption capacity is in the order of BS-PST-10 > BS-PST-5 > BS-PST-1, which indicates an increase of adsorption performance along with BS usage. The amphoteric nature of loaded BS and the additional COO⁻ might be in favor of the adsorption process for NH₄⁺ (Zheng et al., 2012). Among all the three SDS modified samples, only SDS-PST-10 possesses enhanced adsorption

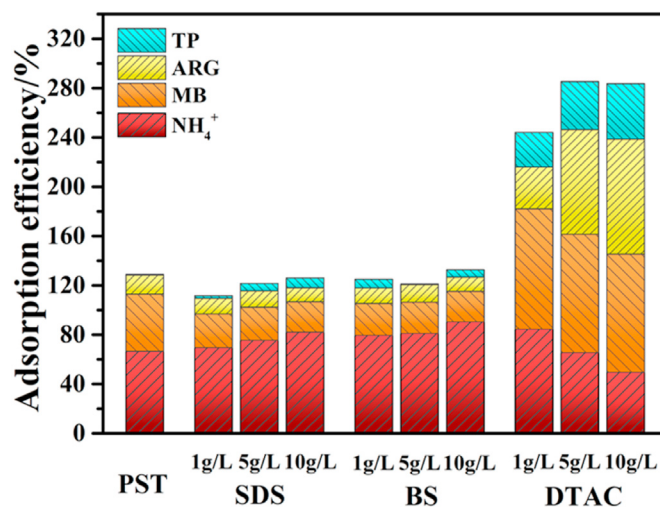


Fig. 1. Effect of surfactants usage dosage on the adsorption behavior of four kinds of representative contaminants at pH = 7.

capacity for NH_4^+ compared with pure PST. The additional Na^+ from 10 g L^{-1} SDS in the modified PST might be beneficial to the ion-exchange with NH_4^+ . The dosage of DTAC makes the greatest influence on the adsorption of NH_4^+ . The adsorption efficiency of NH_4^+ by modified PSTs decreases with the increase of DTAC dosage and is in the order of DTAC-PST-1 > DTAC-PST-5 > DTAC-PST-10. The electrostatic repulsion between NH_4^+ and cationic group ($\text{R}_4\text{-N}^+$) in DTAC and the reduction of Na^+ probably make an explanation for this result.

For the same cationic but organic contaminant MB, the adsorption performance of the modified samples is different from that of NH_4^+ . It is observable that the adsorption capacity of BS-PSTs or SDS-PSTs for MB are worse than that of bare PST. The different adsorption performance of the same modified PST for NH_4^+ and MB demonstrates that the adsorption sites for these two matters are different though they are both cationic contaminants. The DTAC-PSTs performed better than PST in the adsorption of MB whether the dosage is 1, 5 or 10 g L^{-1} , which is probably resulted from the functional groups on the adsorbent surface.

The adsorption capacity of anionic contaminant ARG or phosphate onto PST is low at $\text{pH} = 7$ because of the electrostatic repulsion. After modification, a dramatic increase in adsorption capacity for ARG or phosphate is only observed in DTAC-PSTs. In addition, the adsorption capacity of TP onto DTAC-PSTs increases with the increase of surfactant dosage. The above adsorption results and analysis demonstrate that surfactant modification could affect the adsorption performance of PSTs and DTAC modification could significantly enhance the adsorption capacity for anionic contaminant.

3.3. Effect of pH

The adsorption capacity of four contaminants onto the as-prepared samples at different solution pH were conducted and the results are showed in Fig. S9. It is observable the adsorption capacity of NH_4^+ onto all the samples (PST and the modified samples) are at the similar value among the given pH range (Fig. S9c). However, the adsorption performance of these samples for the cationic contaminant (MB) are in the order of DTAC-PST-5 > PST > BS-PST-5 \approx SDS-PST-5 (Fig. S9a). The modification by cationic surfactant successfully enhanced the adsorption capacity of PST for organic matter. The optimal solution pH for NH_4^+ removal is 3.0, which mainly results from the molecular form of $\text{NH}_4^+\text{-N}$ in alkaline solution. It is interesting that the adsorption capacity of MB onto DTAC-PST-5 maintains in a high level and decreases slightly with the pH, which is opposite to PST. Usually, the uptake of MB from aqueous solution by adsorbent are more effective in alkaline environment due to its cationic nature (Fu et al., 2015; Zhao et al., 2015; Wan et al., 2017b). The enhanced adsorption capacity of DTAC-PST-5 for MB in acidic solution indicates that MB could be adsorbed not only through electrostatic attraction but also others. In addition, the adsorption capacity of anionic ARG and phosphate onto PST at acidic and neutral solution are significantly enhanced by DTAC modification and decreases with the increase of solution pH (Fig. S9b and Fig. S9d). All the results indicate that the cationic surfactant (DTAC) modification could enhance the adsorption ability of bare PST, especially for the removal of anionic contaminants.

3.4. Adsorption kinetics

The kinetic experiments were conducted to find the effect of contact time on the adsorption performance of the samples for cationic and anionic contaminants. It is observable that adsorption equilibrium for all the processes could be reached quickly within

30 min for MB (Fig. 2a), 10 min for ARG (Fig. 2b), 20 min for NH_4^+ (Figs. 2c), and 60 min for TP (Fig. 2d). In addition, the same order of adsorption capacity among all the PSTs as mentioned before is also illustrated from the kinetic adsorption results. These data also indicate that surfactant modification could significantly affect the adsorption performance of bare PST, and DTAC-PST performs well for removal of both cationic and anionic contaminants. The experimental data of these contaminants are fitted to pseudo-first-order, pseudo-second-order and elovich models respectively. The corresponding calculated parameters are determined by the nonlinear equations and listed in Table S6 and Table S7. It is evident that most of the experimental data could be fitted to pseudo-second order model well because the values of coefficient are closer to 1 than pseudo-first order model or elovich model. These results demonstrate that the adsorption of four contaminants on each sample are mainly controlled by chemisorption involving valency forces through the sharing or exchange of electrons as covalent forces, and ion exchange (Ho, 2006). In addition, the adsorption of MB, ARG, NH_4^+ or H_2PO_4^- onto PST, SDS-PST-5 or BS-PST-5 could not be described well by the above models, which demonstrates that the adsorption process is not favorable. The elovich equation assumes that the actual solid surfaces are energetically heterogeneous and interactions between the adsorbed species could substantially affect the kinetics of adsorption at low surface coverage (Sen Gupta and Bhattacharyya, 2011). It is observable that the values of R^2 for elovich model are not close to 1 and indicate that adsorption kinetics is affected by interactions between adsorbates. Hence, the difference of adsorbates during each adsorption process might cause the above different fitting results. However, the difference in adsorption performance before and after modification asks for a detailed study on the adsorption mechanism connected with the surfactant modification.

3.5. Adsorption isotherms

The isotherm adsorption experiment results of each contaminant (NH_4^+ , H_2PO_4^- , MB or ARG) onto DTAC-PST-5 is shown in Fig. S10, respectively. It is evident that the adsorption capacity of all the adsorption process are initial concentration dependent. However, the theoretical maximum adsorption capacity and the adsorption process nature can not be obtained from the finite experimental data. Therefore, the Langmuir model and Freundlich model were applied in the fitting of experimental result. The fitting curves are shown in Fig. S10 and the corresponding parameters are listed in Table S8. The value of coefficient R^2 demonstrated that Langmuir model could describe all the adsorption process better than Freundlich model, which indicated a monolayer adsorption in the contact of contaminants with adsorbent surface. The theoretical maximum adsorption capacity of DTAC-PST-5 for the four adsorbates were calculated as 49.28 mg g^{-1} for NH_4^+ , 34.74 mg g^{-1} for TP, 81.87 mg g^{-1} for MB and 545.81 mg g^{-1} for ARG. The adsorption performance for NH_4^+ , TP, MB or ARG by other reported surfactant modified adsorbents are summarized and listed in Table 1. It is indicated that DTAC-PST-5 could possess satisfactory adsorption capacity for the above contaminants, especially for the anionic chemicals. The versatile adsorption performance according to these results indicate DTAC modified sample a promising adsorbent for complicated wastewater.

3.6. Simultaneous adsorption

In order to evaluate the adsorption performance of samples for all the mentioned contaminants in the same procedure, the simultaneous adsorption experiment was conducted in simulated mixed wastewater. DTAC-PST-1 and DTAC-PST-5 were chosen as

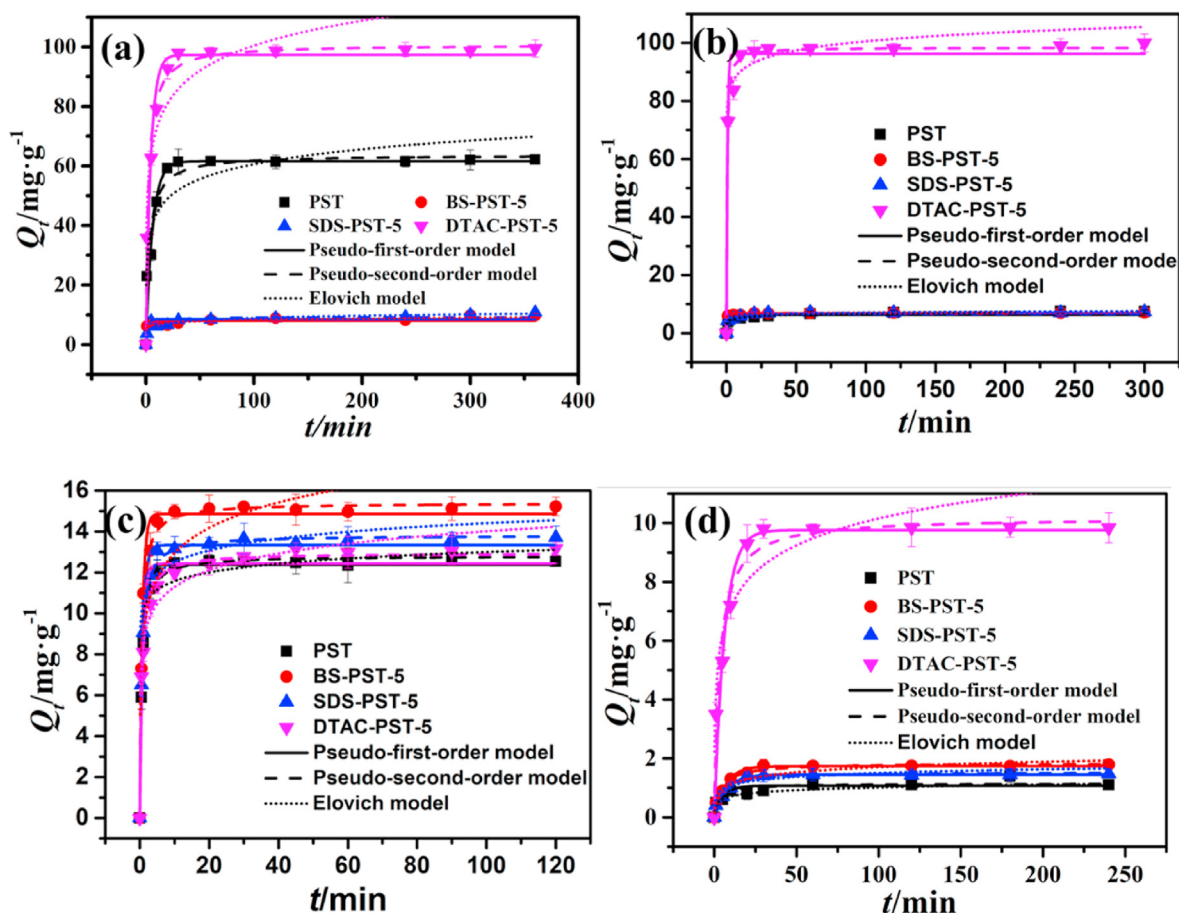


Fig. 2. Relationship between contact time and the adsorption capacity for (a) MB (b) ARG (c) NH_4^+ and (d) TP onto the samples.

Table 1

Adsorption performance for NH_4^+ , TP, MB or ARG by DTAC-PST-5 compared with other reported surfactant modified materials.

Contaminants	Samples	$C_0/\text{mg} \cdot \text{L}^{-1}$	$\text{Dos}/\text{g} \cdot \text{L}^{-1}$	$Q_{\text{max}}/\text{mg} \cdot \text{g}^{-1}$	Reference
NH_4^+	SDS modified activated carbon	30–1000	20	6.7	Lee et al. (2018)
NH_4^+	HDTMA modified zeolite	25–250	20	7.2	Tao et al. (2015)
NH_4^+ , H_2PO_4^-	Cetylpyridinium bromide modified zeolite	NH_4^+ : 25–250 TP: 20–180	20	NH_4^+ : 6.3 TP: 2.4	Li et al. (2017)
NH_4^+ , PO_4^{3-} , MB	HDTMA modified zeolite	NH_4^+ : 5–50 PO_4^{3-} : 5–50 MB: 5–550	5	NH_4^+ : 30.5 PO_4^{3-} : 29.8 MB: 10.3	Xie et al. (2013)
H_2PO_4^-	HDTMA modified clinoptilolite	0–50	100	0.2	Dionisiou et al. (2012)
H_2PO_4^-	HDTMA modified zeolite	7.76–2813	100	0.9	Schick et al. (2011)
PO_4^{3-}	HDTMA modified Akaganeite	10–300	0.5	451	Deliyanni et al. (2007)
H_2PO_4^-	Gemini surfactant modified montmorillonite	0–46.5	0.8	12.1	Luo et al. (2020)
MB	Sodium lauryl sulphate modified activated carbon	0–50	0.15	232.5	Kuang et al. (2020)
MB	SDS modified ZnFe_2O_4	40–100	0.1	699.3	Zhang et al. (2017)
MB	F127 modified mesoporous carbon	50–400	2.5	388.0	Malekbala et al. (2015)
MB	Dodecyl sulfobetaine modified montmorillonite	0–400	1	254.0	Fan et al. (2014)
ARG	HDTMA modified titanate nanotubes	100–2000	1	285.0	Juang et al. (2008)
NH_4^+ , H_2PO_4^- , MB, ARG	DTAC-PST-5	NH_4^+ : 10–120 TP: 3–50 MB: 50–400 ARG: 50–400	2	NH_4^+ : 49.3 TP: 34.7 MB: 81.9 ARG: 545.8	This study

the adsorbent materials in this procedure because DTAC-PST-10 performed poorly in the adsorption of NH_4^+ as shown in Fig. 3. It is illustrated that both the two DTAC-modified samples could maintain adsorption ability for every contaminant even though there are four chemicals in the solution (please see Fig. 3). The safe discharge levels of these contaminants were set according to the

regulation in China (GB, 18918–2002). The adsorption results show that the concentration of all the chemicals could be controlled below the discharge standards at the pH of 3.0 by either DTAC-PST-1 or DTAC-PST-5. Therefore, the adsorption performance of DTAC-PSTs can be adjusted by changing the DTAC dosage in modification according to the initial contaminant concentration in

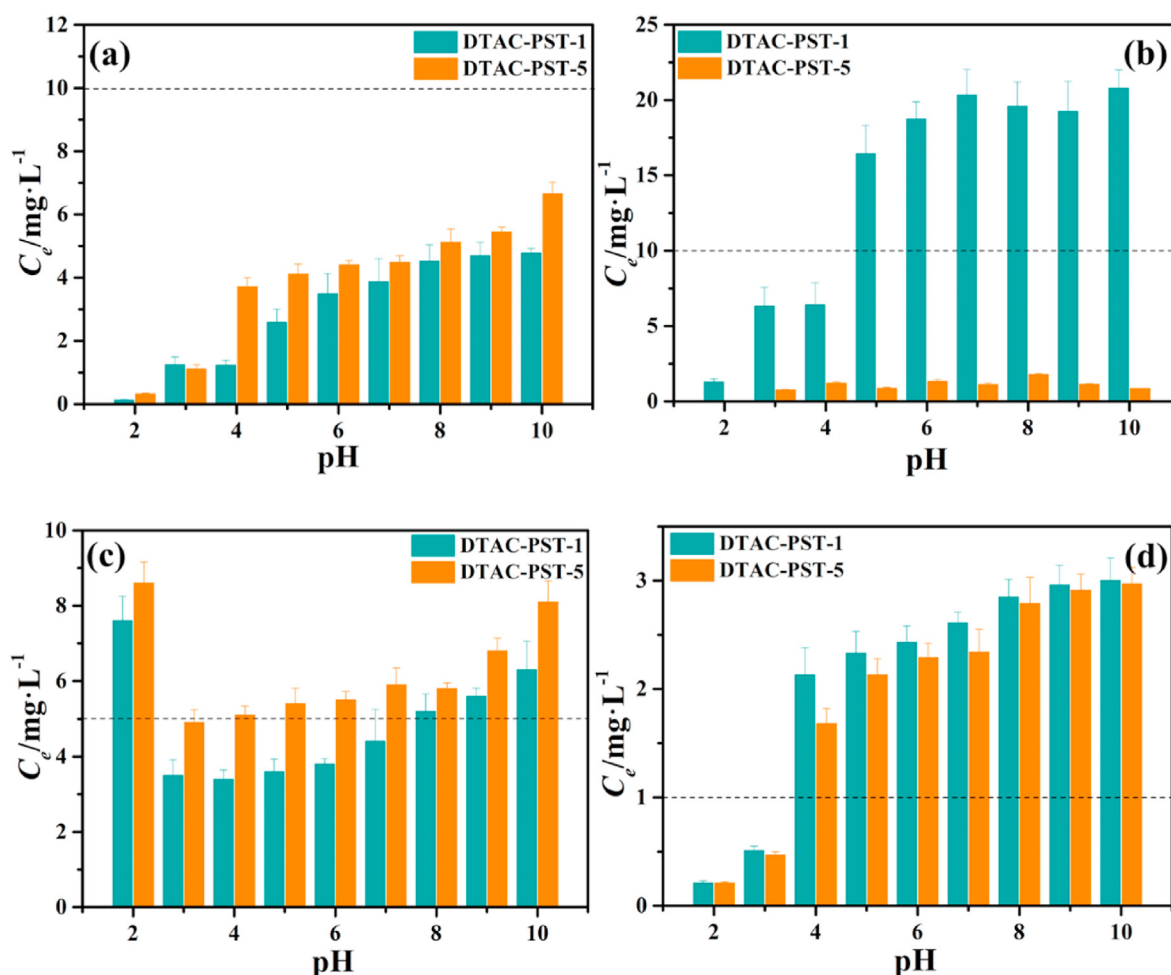


Fig. 3. The equilibrium concentration of simultaneous adsorption of (a) MB, (b) ARG, (c) NH_4^+ and (d) TP onto DTAC-PST-1 and DTAC-PST-5, (the dashed line is the safe discharge levels according to GB, 18918–2002 in China). Experimental conditions: $C_0 = 50 \text{ mg MB}\cdot\text{L}^{-1}$, $50 \text{ mg ARG}\cdot\text{L}^{-1}$, $10 \text{ mg NH}_4^+\cdot\text{L}^{-1}$ and $3 \text{ mg TP}\cdot\text{L}^{-1}$; contact time = 120 min.

wastewater. The DTAC modification could significantly enhance the versatile adsorption ability of PST for the simultaneous removal of cationic and anionic chemicals. The methods to broaden the optimal pH range will be studied in the future.

3.7. Adsorption mechanism

The FTIR spectra of PST and the modified PST samples before and after adsorption of cationic NH_4^+ and MB are presented in Fig. 4. The attribution of these peaks are listed in Table S1–S4. The peak at 1340 cm^{-1} is ascribed to the vibration of Ti–O bond, which is formed through the destruction of Ti–OH by NaOH during the synthesis (Chen et al., 2010; Kiatkittipong et al., 2010; Ye et al., 2013). Ion-exchange between NH_4^+ and Na^+ has been demonstrated as the main adsorption mechanism for titanate-based materials in the removal of NH_4^+ from aqueous solution (Zhang et al., 2019). After the adsorption of NH_4^+ , the peak responding to Ti–O bond of all samples shifts to 1400 cm^{-1} , which could be assigned to the vibration of N–H deformation. (Huang et al., 2014; Zhao et al., 2014; Wang et al., 2017). The phenomenon indicates that the NH_4^+ adsorption on PST, BS-PST-5 and SDS-PST-5 are still dominated by the ion exchange mechanism. For DTAC-PSTs, the FTIR (Fig. 4c) and EDS results illustrate that Na^+ amount declines after the modification, which probably cause the reduction of NH_4^+ adsorption. However, the peak at about 970 cm^{-1} corresponding to

the vibration of C–N⁺ disappears after the adsorption demonstrates that ion exchange might occur between NH_4^+ and positively charged organic N, which makes some contributions for adsorption. In addition, the COO^- groups exist in the structure of BS-PSTs could increase the adsorption sites for cationic ions through charge balance, which eventually enhances the adsorption capacity of BS-PST-5 for NH_4^+ uptake.

For the adsorption of MB, it could be deduced from the peaks like C–N symmetric stretching at 1397 cm^{-1} and aromatic framework vibration at about 1608 cm^{-1} that MB molecules have been successfully adsorbed onto all the samples. Indeed, the formation of PST is a complex process and its surface could be negatively charged gradually with the increase of solution pH (Muehlebach et al., 1970), which is beneficial for the adsorption of cationic MB. Moreover, the bond at 680 cm^{-1} representing the O–O group in PST shifts to 672 cm^{-1} after the adsorption of MB (please see Fig. 4a), which demonstrates that electrostatic interaction was not the sole adsorption interaction. SDS and BS modified PST samples possess more positive surface than PST as shown in Fig. S7, which causes a dramatically reduction in adsorption capacity of MB. It is observable that the peaks related to the groups in DTAC disappear and peaks responding to MB appear instead after the adsorption of MB onto DTAC-PST-5 (Fig. 4c). It is likely that the DTAC molecules on the surface of samples could be exchanged by the cationic MB during the adsorption, which makes an explanation for the

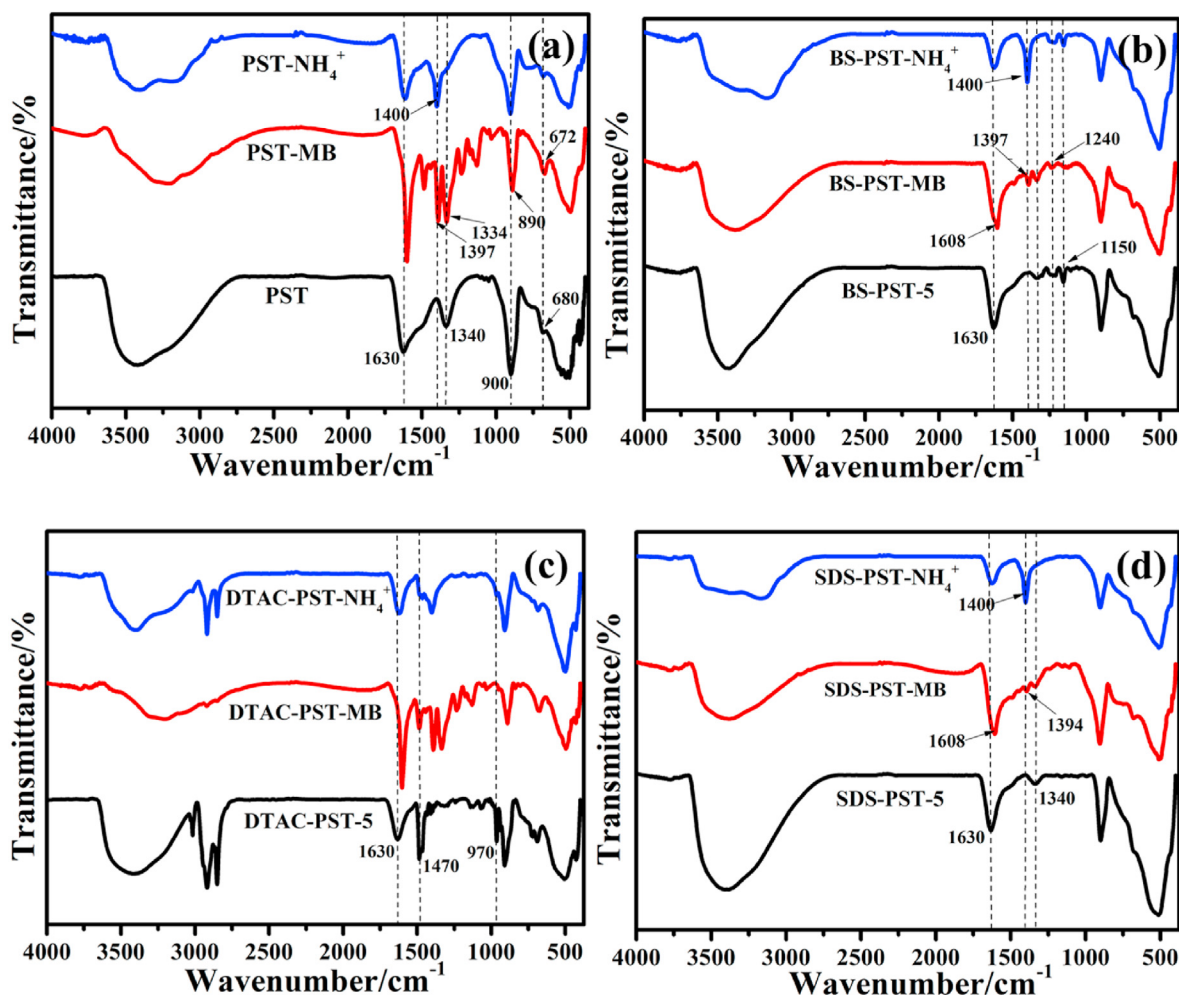


Fig. 4. FT-IR spectra of (a) PST (b) BS-PST-5 (c) DTAC-PST-5 and (d) SDS-PST-5 before and after adsorption of NH_4^+ and MB.

enhancement of adsorption capacity for MB in the acidic solution. The interaction between the PSTs and abundant groups of MB make the newly formed composite stable in solution. The decrease of Na^+ and increase of DTAC-N^+ in the as-prepared samples eventually result in the enhancement of MB adsorption, which indicates that organic MB molecules are tend to exchange with organic ligands prior to inorganic cations.

Titanate-based samples usually exhibit poor adsorption capacity for anionic contaminant because of their negative charged surface in general solution. Herein, the adsorption performance of PST, BS modified and SDS modified PSTs for anionic ARG and H_2PO_4^- are limited as shown in adsorption experiment results. The FT-IR results of these materials after the adsorption also confirm this conclusion for the little change in spectra (Fig. 5). The analysis data of these peaks are listed in Table S5. Nonetheless, the adsorption capacity of ARG or H_2PO_4^- onto DTAC-PSTs are both enhanced by 10 times of those onto the pure PST. Fig. 5c shows the FT-IR spectra of DTAC-PST-5 before and after adsorption to help figure out the adsorption mechanism for anionic contaminants. It is obvious that H_2PO_4^- and ARG have been successfully adsorbed onto DTAC-PST-5 due to the vibration of P=O (1011 cm^{-1}) and S=O (1043 cm^{-1}), respectively (Wang et al., 2015; Deng et al., 2019; Hao et al., 2019). The peaks at 1470 cm^{-1} and 970 cm^{-1} representing the quaternary ammonium C-N $^+$ disappear after the adsorption, which demonstrates that interaction between C-N $^+$ group and anionic molecules are the main driverforce for the removal of anionic chemicals.

In addition, the XPS high resolution results of DTAC-PST before and after adsorption of H_2PO_4^- or ARG are shown in Fig. 6. It is evident that the C1s band of the sample DTAC-PST-5 remained unchanged during the adsorption process, which demonstrated that C related functional groups didn't make contributions for the enhanced adsorption of contaminants. For the O1s high resolution band, the O1s cored at 533.42 eV is described to adsorbed water, the peaks at 531.75 eV can be attributed to Ti-O bond, the peaks at 529.58 eV apply to O-H bonds. It can be observed from Fig. 6 that the amount of O-H group in DTAC-PST-5 increased after the adsorption of P or ARG. In addition, the peaks shifting in O1s during the adsorption indicate that electrostatic attraction occurred, which is consistent with the result of FTIR. The main mechanism of modification and adsorption are illustrated in Fig. 7.

3.8. Adsorption reusability

The stability of DTAC modification was evaluated after washed with deionized water or NaCl solution. The TGA result (Fig. 8a) indicated that the DTAC on PST surface containing first layer and second layer, which is attributed to the different intensity in surface-surfactant interactions (Guan et al., 2010). After washed with deionized water or NaCl solution, about 82.1% and 72.6% surfactant loading remained bound to the PST surface (Fig. 8b and c), which indicated a passable stability or long-term performance of DTAC-PST-5 in aqueous environment. Due to the results in pH

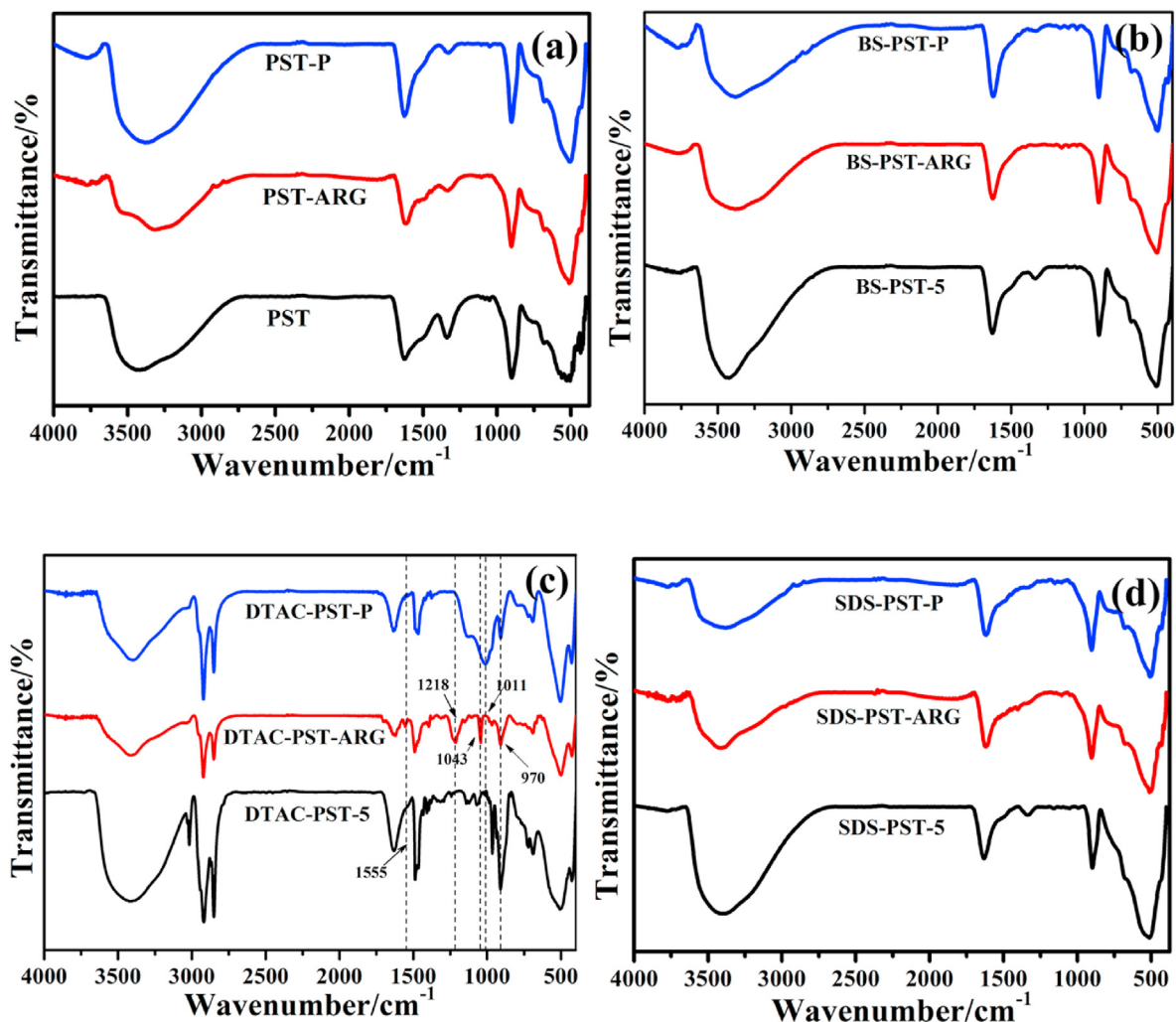


Fig. 5. FT-IR spectra of (a) PST and (b) BS-PST-5 (c) DTAC-PST-5 and (d) SDS-PST-5 before and after adsorption of TP and ARG.

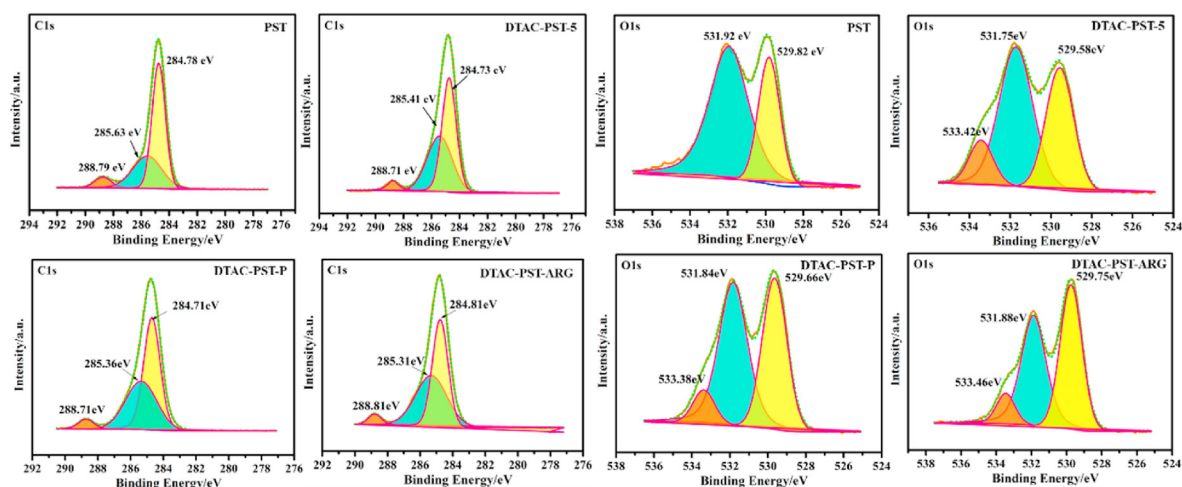


Fig. 6. XPS high resolution of C1s and O1s for PST, DTAC-PST-5, DTAC-PST-P and DTAC-PST-ARG.

experiment, 0.5 mol L⁻¹ NaOH solution was used to recover the exhausted adsorbents. The regenerated adsorbent performed well in the adsorption of mixed contaminants solution and could

maintain at least 80% of the adsorption capacity after five cycles compared to the fresh adsorbent. The above results demonstrate that DTAC-PST possesses a good reusability in the adsorption of

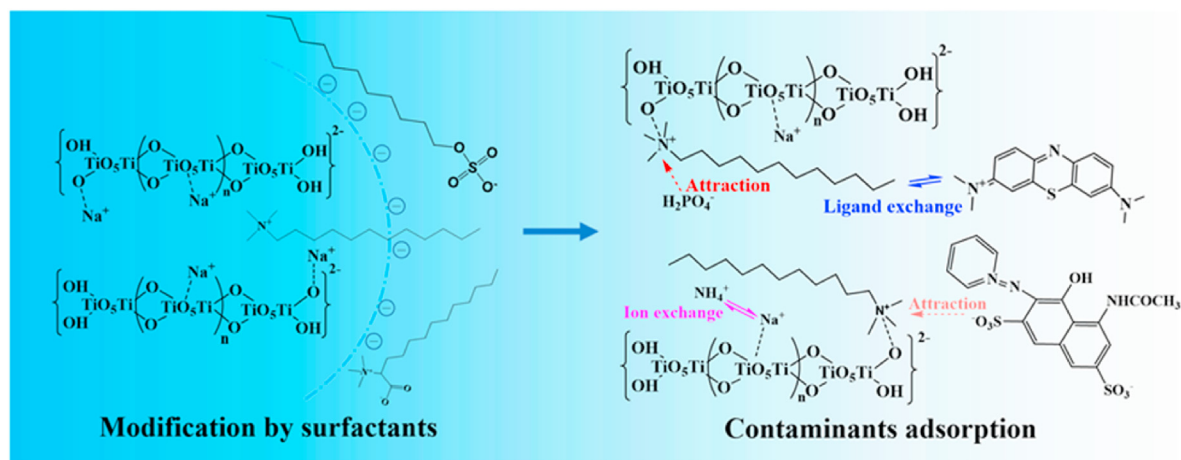


Fig. 7. The modification and adsorption route of PST for four contaminants.

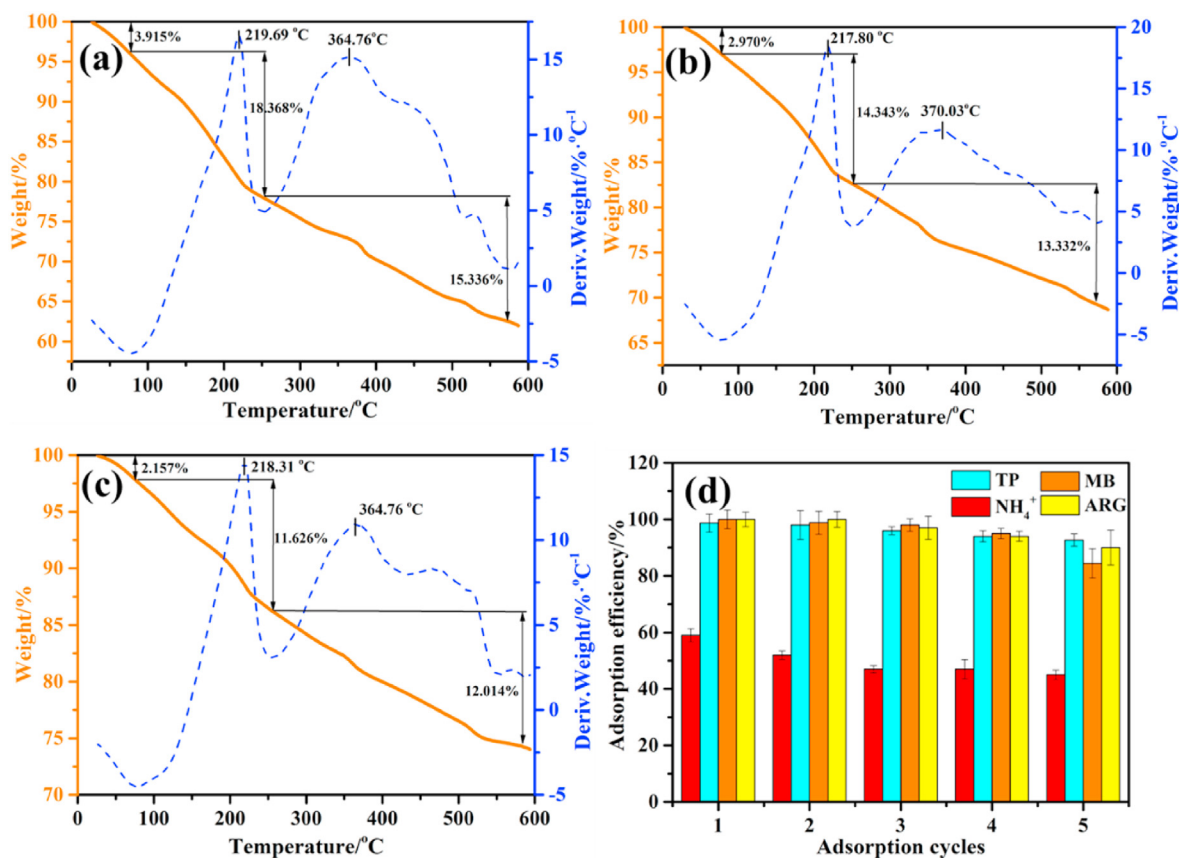


Fig. 8. The TGA results of DTAC-PST-5 (a), DTAC-PST-5 washed with deionized water (b) or NaCl solution (c) for 72 h and reusability of regenerated DTAC-PST-5 (d). Experimental conditions for (d): initial concentration of mixed solution as 10 mg L^{-1} for NH_4^+ , 3 mg L^{-1} for TP, 50 mg L^{-1} for MB and 50 mg L^{-1} for ARG; initial mixed solution pH 3.0; contact time 120 min.

mixed solution containing cationic and anionic contaminants.

4. Conclusion

Surfactants (DTAC, BS, SDS) modified titanate-based materials (PST) were facily synthesized and assessed as the adsorbent for the removal of four typical cationic and anionic contaminants (MB, ARG, NH_4^+ and H_2PO_4^-). The XPS, EDS and FTIR results indicated that

surfactant modification level was in the order of DTAC > BS > SDS. Electrostatic interaction and ion exchange were demonstrated as the main ways for modification. The adsorption performance for every contaminant was surfactant dosage dependent. DTAC-PSTs performed better than PST, BS-PSTs and SDS-PSTs in the removal of MB, ARG and H_2PO_4^- , and maintained the similar adsorption capacity for NH_4^+ as pure PST. The Langmuir calculated maximum adsorption capacity of DTAC-PST-5 is 49.28 mg g^{-1} for NH_4^+ ,

34.74 mg g⁻¹ for TP, 81.87 mg g⁻¹ for MB and 545.81 mg g⁻¹ for ARG. The simultaneous adsorption experiment showed that the DTAC modified PST can control all the four chemical concentrations below the discharge standard (GB, 18918–2002 in China) at the solution pH of 3.0, which suggested DTAC modification is a promising method to enhance the versatile adsorption performance of PSTs for the increasing complex effluent. Ion exchange and ligand exchange are the main mechanism for NH₄⁺ and MB removal, respectively. C–N⁺ group in DTAC–PST made the main contribution to the enhancement of adsorption capacity for anionic ARG and H₂PO₄⁻. In addition, the exhausted DTAC–PST could be desorbed and regenerated by 0.5 mol L⁻¹ NaOH solution and reused at least for five cycles. All the above results indicated that surfactant modification can affect the adsorption performance of PST for different contaminant in wastewater depending on the surfactants species and dosage. DTAC modified PST is a promising adsorbent for versatile adsorption.

Credit author statement

Wenlong Zhang: Conceptualization; Methodology; Formal analysis; Investigation; Writing – original draft, Xiaoyan Yang: Software; Visualization, Changzheng Lin: Validation; Investigation, Jiangtao Feng: Resources; Data curation; Writing – review & editing; Funding acquisition, Hongjie Wang: Writing – review & editing, Wei Yan: Resources; Supervision; Project administration; Funding acquisition.

Declaration of competing interest

The authors declare that they have no known competing financial interests or personal relationships that could have appeared to influence the work reported in this paper.

Acknowledgements

This research is supported by National Natural Science Foundation of China (NO.51978569 and NO.51778054) and the Major Science Technology Program for Water Pollution Control and Treatment of China (NO.2018ZX07110).

Appendix A. Supplementary data

Supplementary data to this article can be found online at <https://doi.org/10.1016/j.chemosphere.2020.129383>.

References

- Chen, Y.C., Lo, S.L., Kuo, J., 2010. Pb(II) adsorption capacity and behavior of titanate nanotubes made by microwave hydrothermal method. *Colloids Surf., A* 361, 126–131.
- Crini, G., Lichtfouse, E., Wilson, L.D., Morin-Crini, N., 2018. Conventional and non-conventional adsorbents for wastewater treatment. *Environ. Chem. Lett.* 17, 195–213.
- Deliyanni, E., Peleka, E., Lazaridis, N., 2007. Comparative study of phosphates removal from aqueous solutions by nanocrystalline akaganéite and hybrid surfactant-akaganéite. *Separ. Purif. Technol.* 52, 478–486.
- Deng, Y., Zhang, T., Sharma, B.K., Nie, H., 2019. Optimization and mechanism studies on cell disruption and phosphorus recovery from microalgae with magnesium modified hydrochar in assisted hydrothermal system. *Sci. Total Environ.* 646, 1140–1154.
- Dionisiou, N.S., Matsi, T., Misopolinos, N.D., 2012. Phosphorus adsorption-desorption on a surfactant-modified natural zeolite: a laboratory study. *Water, Air, Soil Pollut.* 224.
- El Hanache, L., Lebeau, B., Nouali, H., Toufaily, J., Hamieh, T., Daou, T.J., 2019. Performance of surfactant-modified *BEA-type zeolite nanosponges for the removal of nitrate in contaminated water: effect of the external surface. *J. Hazard Mater.* 364, 206–217.
- Fan, H., Zhou, L., Jiang, X., Huang, Q., Lang, W., 2014. Adsorption of Cu²⁺ and methylene blue on dodecyl sulfobetaine surfactant-modified montmorillonite. *Appl. Clay Sci.* 95, 150–158.
- Fu, F., Wang, Q., 2011. Removal of heavy metal ions from wastewaters: a review. *J. Environ. Manag.* 92, 407–418.
- Fu, J., Chen, Z., Wang, M., Liu, S., Zhang, J., Zhang, J., Han, R., Xu, Q., 2015. Adsorption of methylene blue by a high-efficiency adsorbent (polydopamine microspheres): kinetics, isotherm, thermodynamics and mechanism analysis. *Chem. Eng. J.* 259, 53–61.
- Guan, H., Bestland, E., Zhu, C., Zhu, H., Albertsdottir, D., Hutson, J., Simmons, C.T., Ginic-Markovic, M., Tao, X., Ellis, A.V., 2010. Variation in performance of surfactant loading and resulting nitrate removal among four selected natural zeolites. *J. Hazard Mater.* 183, 616–621.
- Hao, H., Wang, Y., Shi, B., 2019. NaLa(CO₃)₂ hybridized with Fe₃O₄ for efficient phosphate removal: synthesis and adsorption mechanistic study. *Water Res.* 155, 1–11.
- He, Y.H., Lin, H., Dong, Y.B., Liu, Q.L., Wang, L., 2016. Simultaneous removal of ammonium and phosphate by alkaline-activated and lanthanum-impregnated zeolite. *Chemosphere* 164, 387–395.
- Ho, Y.S., 2006. Review of second-order models for adsorption systems. *J. Hazard Mater.* 136, 681–689.
- Hokkanen, S., Bhatnagar, A., Sillanpää, M., 2016. A review on modification methods to cellulose-based adsorbents to improve adsorption capacity. *Water Res.* 91, 156–173.
- Huang, H., Xiao, D., Pang, R., Han, C., Ding, L., 2014. Simultaneous removal of nutrients from simulated swine wastewater by adsorption of modified zeolite combined with struvite crystallization. *Chem. Eng. J.* 256, 431–438.
- Juang, L., Lee, C., Wang, C., Hung, S., Lyu, M., 2008. Adsorptive removal of acid red 1 from aqueous solution with surfactant modified titanate nanotubes. *Environ. Eng. Sci.* 25, 519–528.
- Kiatkittipong, K., Ye, C., Scott, J., Amal, R., 2010. Understanding hydrothermal titanate nanoribbon formation. *Cryst. Growth Des.* 10, 3618–3625.
- Kuang, Y., Zhang, X., Zhou, S., 2020. Adsorption of methylene blue in water onto activated carbon by surfactant modification. *Water* 12.
- Lee, W., Yoon, S., Choe, J.K., Lee, M., Choi, Y., 2018. Anionic surfactant modification of activated carbon for enhancing adsorption of ammonium ion from aqueous solution. *Sci. Total Environ.* 639, 1432–1439.
- Li, C., Yao, J., Zhang, T.C., Xing, W., Liang, Y., Xiang, M., 2017. Simultaneous removal of nitrogen and phosphorus by cetylpyridinium bromide modified zeolite. *Water Sci. Technol.* 76, 2895–2906.
- Li, H., Wu, W., Hao, X., Wang, S., You, M., Han, X., Zhao, Q., Xing, B., 2018a. Removal of ciprofloxacin from aqueous solutions by ionic surfactant-modified carbon nanotubes. *Environ. Pollut.* 243, 206–217.
- Li, Y., Hu, X., Liu, X., Zhang, Y., Zhao, Q., Ning, P., Tian, S., 2018b. Adsorption behavior of phenol by reversible surfactant-modified montmorillonite: mechanism, thermodynamics, and regeneration. *Chem. Eng. J.* 334, 1214–1221.
- Li, Y., Yin, X., Huang, X., Tian, J., Wu, W., Liu, X., 2019. The novel and facile preparation of 2DMoS₂@C composites for dye adsorption application. *Appl. Surf. Sci.* 495, 143626.
- Liu, C., Wu, P., Zhu, Y., Tran, L., 2016. Simultaneous adsorption of Cd²⁺ and BPA on amphoteric surfactant activated montmorillonite. *Chemosphere* 144, 1026–1032.
- Luo, W., Huang, Q., Zhang, X., Antwi, P., Mu, Y., Zhang, M., Xing, J., Chen, H., Ren, S., 2020. Lanthanum/Gemini surfactant-modified montmorillonite for simultaneous removal of phosphate and nitrate from aqueous solution. *J. Water Process. Eng.* 33, 101036.
- Malekbala, M.R., Khan, M.A., Hosseini, S., Abdullah, L.C., Choong, T.S.Y., 2015. Adsorption/desorption of cationic dye on surfactant modified mesoporous carbon coated monolith: equilibrium, kinetic and thermodynamic studies. *J. Ind. Eng. Chem.* 21, 369–377.
- Muehlebach, J., Mueller, K., Schwarzenbach, G., 1970. Peroxo complexes of titanium. *Inorg. Chem.* 9, 2381–2390.
- Rajapaksha, A.U., Chen, S.S., Tsang, D.C., Zhang, M., Vithanage, M., Mandal, S., Gao, B., Bolan, N.S., Ok, Y.S., 2016. Engineered/designer biochar for contaminant removal/immobilization from soil and water: potential and implication of biochar modification. *Chemosphere* 148, 276–291.
- Schick, J., Caillet, P., Paillaud, J.-L., Patarin, J., Freitag, S., Mangold-Callarec, C., 2011. Phosphate uptake from water on a surfactant-modified zeolite and ca-zeolites. *J. Porous Mater.* 19, 405–414.
- Schindler, D.W., Carpenter, S.R., Chapra, S.C., Hecky, R.E., Orihel, D.M., 2016. Reducing phosphorus to curb lake eutrophication is a success. *Environ. Sci. Technol.* 50, 8923–8929.
- Schwarzenbach, R.P., Egli, T., Hofstetter, T.B., von Gunten, U., Wehrli, B., 2010. Global water pollution and human health. *Annu. Rev. Environ. Resour.* 35, 109–136.
- Sen Gupta, S., Bhattacharyya, K.G., 2011. Kinetics of adsorption of metal ions on inorganic materials: a review. *Adv. Colloid Interface Sci.* 162, 39–58.
- Shayesteh, H., Rahbar-Kelishami, A., Norouzbegi, R., 2016. Evaluation of natural and cationic surfactant modified pumice for Congo red removal in batch mode: kinetic, equilibrium, and thermodynamic studies. *J. Mol. Liq.* 221, 1–11.
- Shen, Y., Chen, B., 2015. Sulfonated graphene nanosheets as a superb adsorbent for various environmental pollutants in water. *Environ. Sci. Technol.* 49, 7364–7372.
- Shi, B., Zhao, C., Ji, Y., Shi, J., Yang, H., 2020. Promotion effect of PANI on Fe-PANI/Zeolite as an active and recyclable Fenton-like catalyst under near-neutral condition. *Appl. Surf. Sci.* 508, 145298.
- Si, Q., Zhu, Q., Xing, Z., 2018. Simultaneous removal of nitrogen and phosphorus by magnesium-modified calcium silicate core-shell material in water. *Ecotoxicol.*

- Environ. Saf. 163, 656–664.
- Tan, X., Fang, M., Tan, L., Liu, H., Ye, X., Hayat, T., Wang, X., 2018. Core-shell hierarchical $\text{C@Na}_2\text{Ti}_3\text{O}_7 \cdot 9\text{H}_2\text{O}$ nanostructures for the efficient removal of radionuclides. *Environ.-Sci. Nano* 5, 1140–1149.
- Tang, L., Wang, J., Wang, L., Jia, C., Lv, G., Liu, N., Wu, M., 2016. Facile synthesis of silver bromide-based nanomaterials and their efficient and rapid selective adsorption mechanisms toward anionic dyes. *ACS Sustain. Chem. Eng.* 4, 4617–4625.
- Tao, Q., Hu, M., Ma, X., Xiang, M., Zhang, T.C., Li, C., Yao, J., Liang, Y., 2015. Simultaneous removal of ammonium and nitrate by HDTMA-modified zeolite. *Water Sci. Technol.* 72, 1931–1939.
- Turki, A., Kochkar, H., Guillard, C., Berhault, G., Ghorbel, A., 2013. Effect of Na content and thermal treatment of titanate nanotubes on the photocatalytic degradation of formic acid. *Appl. Catal., B* 138–139, 401–415.
- Wan, C., Ding, S., Zhang, C., Tan, X., Zou, W., Liu, X., Yang, X., 2017a. Simultaneous recovery of nitrogen and phosphorus from sludge fermentation liquid by zeolite adsorption: mechanism and application. *Separ. Purif. Technol.* 180, 1–12.
- Wan, X., Zhan, Y., Long, Z., Zeng, G., He, Y., 2017b. Core@double-shell structured magnetic halloysite nanotube nano-hybrid as efficient recyclable adsorbent for methylene blue removal. *Chem. Eng. J.* 330, 491–504.
- Wang, H., Wang, X., Xia, P., Song, J., Ma, R., Jing, H., Zhang, Z., Cheng, X., Zhao, J., 2017. Eco-friendly synthesis of self-existed magnesium oxide supported nanorod-like palygorskite for enhanced and simultaneous recovery of nutrients from simulated wastewater through adsorption and in-situ struvite formation. *Appl. Clay Sci.* 135, 418–426.
- Wang, L., Cao, Y., 2018. Adsorption behavior of phenanthrene on CTAB-modified polystyrene microspheres. *Colloids Surf., A* 553, 689–694.
- Wang, L., Ni, X., Cao, Y., Cao, G., 2018a. Adsorption behavior of bisphenol A on CTAB-modified graphite. *Appl. Surf. Sci.* 428, 165–170.
- Wang, L., Wang, J., Wang, Z., He, C., Lyu, W., Yan, W., Yang, L., 2018b. Enhanced antimonate (Sb(V)) removal from aqueous solution by La-doped magnetic biochars. *Chem. Eng. J.* 354, 623–632.
- Wang, L., Wang, J., Yan, W., He, C., Shi, Y., 2020. MgFe_2O_4 -biochar based lanthanum alginate beads for advanced phosphate removal. *Chem. Eng. J.* 387, 123305.
- Wang, M., Xie, R., Chen, Y., Pu, X., Jiang, W., Yao, L., 2018c. A novel mesoporous zeolite-activated carbon composite as an effective adsorbent for removal of ammonia-nitrogen and methylene blue from aqueous solution. *Bioresour. Technol.* 268, 726–732.
- Wang, N., Li, J., Lv, W., Feng, J., Yan, W., 2015. Synthesis of polyaniline/ TiO_2 composite with excellent adsorption performance on acid red G. *RSC Adv.* 5, 21132–21141.
- Wang, S., Peng, Y., 2010. Natural zeolites as effective adsorbents in water and wastewater treatment. *Chem. Eng. J.* 156, 11–24.
- Wang, T., Zhao, P., Lu, N., Chen, H., Zhang, C., Hou, X., 2016. Facile fabrication of $\text{Fe}_3\text{O}_4/\text{MIL-101}(\text{Cr})$ for effective removal of acid red 1 and orange G from aqueous solution. *Chem. Eng. J.* 295, 403–413.
- Xie, Q., Xie, J., Chi, L., Li, C., Wu, D., Zhang, Z., Kong, H., 2013. A new sorbent that simultaneously sequesters multiple classes of pollutants from water: surfactant modified zeolite. *Sci. China Technol. Sci.* 56, 1749–1757.
- Xu, D., Cao, J., Li, Y., Howard, A., Yu, K., 2019. Effect of pyrolysis temperature on characteristics of biochars derived from different feedstocks: a case study on ammonium adsorption capacity. *Waste Manag.* 87, 652–660.
- Xu, Q., Li, W., Ma, L., Cao, D., Owens, G., Chen, Z., 2020. Simultaneous removal of ammonia and phosphate using green synthesized iron oxide nanoparticles dispersed onto zeolite. *Sci. Total Environ.* 703, 135002.
- Ye, C., Yan, B., Ji, X., Liao, B., Gong, R., Pei, X., Liu, G., 2019. Adsorption of fluoride from aqueous solution by fly ash cenospheres modified with paper mill lime mud: experimental and modeling. *Ecotoxicol. Environ. Saf.* 180, 366–373.
- Ye, M.M., Lu, Z.D., Hu, Y.X., Zhang, Q., Yin, Y.D., 2013. Mesoporous titanate based cation exchanger for efficient removal of metal cations. *J. Mater. Chem. A* 1, 5097–5104.
- Yu, R., Shi, Y., Yang, D., Liu, Y., Qu, J., Yu, Z.Z., 2017. Graphene oxide/chitosan aerogel microspheres with honeycomb-cobweb and radially oriented microchannel structures for broad-spectrum and rapid adsorption of water contaminants. *ACS Appl. Mater. Interfaces* 9, 21809–21819.
- Zhang, P., Lo, I., O'Connor, D., Pehkonen, S., Cheng, H., Hou, D., 2017. High efficiency removal of methylene blue using SDS surface-modified ZnFe_2O_4 nanoparticles. *J. Colloid Interface Sci.* 508, 39–48.
- Zhang, W., Fu, R., Wang, L., Zhu, J., Feng, J., Yan, W., 2019. Rapid removal of ammonia nitrogen in low-concentration from wastewater by amorphous sodium titanate nano-particles. *Sci. Total Environ.* 668, 815–824.
- Zhao, R., Wang, Y., Li, X., Sun, B., Wang, C., 2015. Synthesis of beta-cyclodextrin-based electrospun nanofiber membranes for highly efficient adsorption and separation of methylene blue. *ACS Appl. Mater. Interfaces* 7, 26649–26657.
- Zhao, T.H., Tang, Z., Zhao, X.L., Zhang, H., Wang, J.Y., Wu, F.C., Giesy, J.P., Shi, J., 2019. Efficient removal of both antimonite (Sb(III)) and antimonate (Sb(V)) from environmental water using titanate nanotubes and nanoparticles. *Environ.-Sci. Nano* 6, 834–850.
- Zhao, X., Huang, J., Wang, B., Bi, Q., Dong, L., Liu, X., 2014. Preparation of titanium peroxide and its selective adsorption property on cationic dyes. *Appl. Surf. Sci.* 292, 576–582.
- Zheng, Y., Xie, Y., Wang, A., 2012. Rapid and wide pH-independent ammonium-nitrogen removal using a composite hydrogel with three-dimensional networks. *Chem. Eng. J.* 179, 90–98.
- Zhuang, J., Zhang, B., Wang, Q., Guan, S., Li, B., 2019. Construction of novel $\text{ZnTiO}_3/\text{g-C}_3\text{N}_4$ heterostructures with enhanced visible light photocatalytic activity for dye wastewater treatment. *J. Mater. Sci. Mater. Electron.* 30, 6322–6334.